Disturbance observer based sliding mode control for unmanned helicopter hovering operations in presence of external disturbances

Ihsan ULLAH[1,2,3], Hai-Long PEI*[,1,2,3]

*Corresponding author
[1]Key Lab of Autonomous Systems and Networked Control, Ministry of Education, Guangzhou Guangdong 510640, China,
[2]School of Automation, South China University of Technology, Guangzhou Guangdong 510640, China,
[3]Unmanned System Engineering Center of Guangdong Province, a_ihsanullah@yahoo.com, auhlpei@scut.edu.cn*

Abstract: Numerous control techniques are developed for miniature unmanned helicopters to do hover operation with each method having its own advantages and limitations. During the hover operation helicopters suffer from unknown external disturbances such as wind and ground effect. For a stable operation, these disturbances must be compensated accurately. This paper presents a disturbance observer based sliding mode control technique for small-scale unmanned helicopters to do hover operation in presence of external disturbances. To counteract both matched and mismatched uncertainties a new sliding surface is designed based on the disturbances estimations. The controller design is based on the linearized state-space model of the helicopter which effectively describes helicopter dynamics during the hover operations. The model mismatch and external disturbances are estimated as lumped disturbances and are compensated in the controller design. The proposed controller reduces chattering and is capable of handling matched and mismatched uncertainties. The control performance is successfully tested in Simulink.

Key Words: Unmanned helicopter, External Disturbances, Sliding mode control, Disturbance Observer, Chatter reduction, Mismatched uncertainty

I. INTRODUCTION

Miniature helicopters are highly unstable, agile, nonlinear under-actuated system with significant inter-axis dynamic coupling. They are considered to be much more unstable than fixed-wing unmanned air vehicles, and constant control action is required at all times. However, helicopters are highly flexible aircraft, having the ability to hover, maneuvers accurately and carry heavy loads relative to their own weight [1]. Fixed wing aircraft are used for application in favorable non-hostile conditions but in adverse conditions, agile miniature helicopters become a necessity. The conditions where a helicopter can perform better than fixed-wing UAVs include military investigation, bad weather, firefighting, search and rescue, accessing remote locations and ship operations. In such conditions, helicopters are subjected to unknown external disturbances such as wind and ground effect. These

external disturbances have a significant opposing effect on helicopter stability and can have disastrous results in extreme cases. So it is essential to design a controller for the helicopter which can effectively reject the effect of these unknown external disturbances.

In last two decades, there is substantial research about helicopter control problem. Early results showed that classical control methods using Single-Input Single-Output feedback loops for each input exhibit moderate performance since they are unable to coup with the highly coupled multivariable dynamics of the helicopter [2]. Control schemes typically used to maintain stable control of helicopters include PID [3], Linear Quadratic Regulator (LQR) and Linear Quadratic Gaussian (LQG) [4], H_2 [5], H_∞ [6-7]. The majority of linear controllers designed for unmanned helicopter are based on the H∞ method. In [8] an H_∞ static output feedback control design method was proposed for the stabilization of a miniature unmanned helicopter at hover. An interesting comparative study between several control methods is given in [9], [10]. Disturbance Observer-based control techniques are used in [11], [12], [13], [14]. In [14] a direct feed-through simultaneous state and disturbance observer is used where the control and observer gains are obtained using H∞ synthesis but in presence of external disturbances, there is steady state error in helicopter translational dynamics. In [15], [16] back-stepping control design techniques are used for linear tracking control of miniature helicopter without considering external disturbances, the control design is based on the linearized model of helicopter and shows good results in X-plane flight simulator. In [17] sliding mode control via disturbance observer is used for controlling magnetic levitation suspension system. The experimental results showed that the proposed method have excellent robustness in presence of both matched and mismatched uncertainties. In this paper, a disturbance observer based sliding mode control design method (DOB-SMC) is proposed for small-scale unmanned helicopters to do hover operation in presence of external disturbances via a disturbance observer (DOB). The controller design is based on the linearized state-space model of the helicopter. As in [15], [16], [18], [19] the linearized model of the helicopter can be divided into two subsystems, such as the longitudinal-lateral subsystem and the heading-heave subsystem. As there is no strong coupling between the two subsystems at hover and limited by the scope of the paper, for hovering only the longitudinal-lateral dynamics are considered for designing the control law. To counteract both matched and mismatched uncertainties a new sliding surface is designed based on the disturbance estimation. The model mismatch and external distances are estimated as lumped disturbances and are compensated in the controller design. In [17] the proposed method was applied to SISO MAGLEV system but in this paper, its applied to a multivariable under-actuated unmanned helicopter. The rotor flapping dynamics are approximated by the steady-state dynamics of the main rotor which help reducing controller order. The proposed control methods have three attractive features. First, it's insensitive to mismatched uncertainties. Second, the chattering problem is substantially reduced as the switching gain is only required to be greater than the bound on the disturbance estimation error of observer instead of lumped disturbance. Third, the proposed controller has better performance than a traditional SMC in the absence of external disturbances. Simulink simulation has demonstrated successful performance of the proposed controller.

The rest of the paper is organized as follows: A complete nonlinear model of the helicopter and the linearized model at hover condition is presented in section 2. DOB to approximate lumped disturbances during hover is presented in section 3. The proposed controller is derived in details in section 4. Simulation results are given in section 5 and finally concluding remarks are given in section 6.

2. HELICOPTER MODEL

a) Nonlinear Dynamics of Helicopter

The general 11 state nonlinear model [20] of the miniature unmanned helicopter is given as

$$\dot{u} = vr - wq - g\sin\theta + X_{mr}/m + d_{w1}$$
$$\dot{v} = wp - ur + g\sin\emptyset\cos\theta + Y_{mr}/m + d_{w2}$$
$$\dot{w} = uq - vp + g\cos\emptyset\cos\theta + Z_{mr}/m + d_{w3}$$
$$\dot{\emptyset} = p + (\sin\emptyset\tan\theta)q + (\cos\emptyset\tan\theta)r$$
$$\dot{\theta} = (\cos\emptyset)q - (\sin\emptyset)r$$
$$\dot{\varphi} = \sin\emptyset/\cos\theta + \cos\emptyset/\cos\theta \tag{1}$$
$$\dot{p} = qr(I_{yy} - I_{zz})/I_{xx} + L_{mr}/I_{xx} + d_{w4}$$
$$\dot{q} = pr(I_{zz} - I_{xx})/I_{yy} + M_{mr}/I_{yy} + d_{w5}$$
$$\dot{r} = N_v v + N_p p + N_w w + N_r r + N_{ped}.u_{ped} + N_{col}.u_{col} + d_{mm} + d_{w6}$$
$$\dot{a} = -q - 1/t_f.a + A_b.b + A_{lon}.u_{lon} + A_{lat}.u_{lat}$$
$$\dot{b} = -p - 1/t_f.b + B_a.a + B_{lon}.u_{lon} + B_{lat}.u_{lat}$$

where $\boldsymbol{x} = [u\ v\ w\ \emptyset\ \theta\ \varphi\ p\ q\ r\ a\ b]^T$ is the vector of state variable all available for measurement except a and b; u, v and w represents linear velocities in longitudinal, lateral and vertical direction respectively; m is mass of helicopter, g represents acceleration due to gravity; p, q and r represents angular velocities in roll, pitch and yaw axis respectively; $\emptyset, \theta$ and φ are Euler angles of roll, pitch and yaw axes; $\boldsymbol{u}_c(t) = [u_{lon}\ \ u_{lat}\ \ u_{col}\ \ u_{ped}]^T$ is the control input vector; $\boldsymbol{d}_{wi}\ \forall\ i = 1,2,\cdots 6$ are unknown external wind disturbances effecting linear as well as rotational dynamics of helicopter; I_{xx}, I_{yy} and I_{zz} are the rolling moment of inertia, pitching moment of inertia and yawing moment of inertia respectively; a and b are flapping angles of tip-path-plane(TPP) in longitudinal and lateral direction respectively X_{mr}, Y_{mr} and Z_{mr} are the force components of main rotor trust along x, y and z axis; L_{mr} and M_{mr} are roll and pitch moments generated by main rotor. And $\dot{r}$ represents linearized yaw dynamics at hover so d_{mm} is added for the unknown model mismatch at non hover flights; N_v, N_p, N_w and N_r are helicopter stability derivatives and N_{ped} and N_{col} are input derivatives of yaw dynamics identified as in [16]; t_f is flapping time constant; B_a, B_{lat} and B_{lon} are lateral flapping derivatives; A_b, A_{lon} and A_{lat} are longitudinal flapping derivatives. A diagram showing the directions of the helicopter body fixed coordinate system is given in fig. 1.
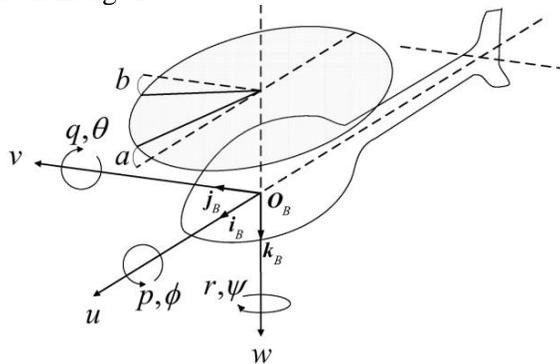
Figure 1. Helicopter body-fixed coordinate system [15]

The force components generated by the main rotor trust in x, y and z direction are given as

$$
\begin{aligned}
X_{mr} &= -T sina \\
Y_{mr} &= T sinb \\
Z_{mr} &= -T cosa\, cosb
\end{aligned}
\tag{2}
$$

where T is the total trust generated by the main rotor. The moments generated by the main rotor along the x and y direction are calculated as

$$
\begin{aligned}
L_{mr} &= \left(k_\beta + T.h_{mr}\right) sinb \\
M_{mr} &= \left(k_\beta + T.h_{mr}\right) sina
\end{aligned}
\tag{3}
$$

where k_β is the torsional stiffness of the main rotor hub; h_{mr} main rotor hub height above the center of gravity of helicopter.

Trust of the main rotor is calculated by iteratively solving the equations of trust and the induced inflow velocity [21].

$$
\begin{aligned}
T &= (w_b - v_i)\frac{\rho \Omega R^2 C_{l\alpha}^m b_m c_m}{4} \\
v_i^2 &= \sqrt{\left(\frac{\bar{v}^2}{2}\right)^2 + \left(\frac{T}{2\rho\pi R^2}\right)^2} - \frac{\bar{v}^2}{2} \\
\bar{v}^2 &= u^2 + v^2 + w(w - 2v_i) \\
w_b &= w + \frac{2}{3}\Omega R k_a k_{col} u_{col}
\end{aligned}
\tag{4}
$$

where v_i is the induced inflow velocity; Ω is rotational speed of the main rotors; ρ is air density; R is main rotor radius; b_m is the number of main rotor blades; c_m is the chord length of the main rotor; $C_{l\alpha}^m$ is coefficient of lift curve slope of the main rotor; k_a is Control gain of the servo actuator; k_{col} is linkage gain from collective actuator to the main blade.

b) Linearized State Space Model at Hover

To derive the control law, the nonlinear model (1) of the helicopter is linearized at hover condition as

$$
\begin{aligned}
\dot{x} &= Ax + Bu_c + Ed_t \\
y &= Cx
\end{aligned}
\tag{5}
$$

At hover condition, the longitudinal-lateral and heading-heave dynamics of the helicopter are weakly coupled with each other and are expressed as two separate sub-systems [14], [16].

$$
\begin{aligned}
\dot{x}_2 &= A_{21}x_1 + A_{22}x_2 + B_{22}u_{c2} + E_{22}d_{t2} \\
y_1 &= C_1 x_1
\end{aligned}
\tag{6}
$$

$$
\begin{aligned}
\dot{x}_1 &= A_{11}x_1 + B_{11}u_{c1} + E_{11}d_{t1} \\
y_2 &= C_2 x_2
\end{aligned}
\tag{7}
$$

where (6) represents longitudinal-lateral subsystem and (7) represents the heading-heave subsystem, $x_1 = [u\ v\ \theta\ \emptyset\ q\ p\ a\ b\ ]^T$, $u_{c1} = [u_{lon}\ u_{lat}]^T$, $d_{t1} = [d_{t1}\ d_{t2}\ d_{t3}\ d_{t4}\ d_{t5}\ d_{t6}\ 0\ 0\ ]^T$, E_{11} is 8×8 identity matrix, $x_2 = [\varphi\ r\ w\ ]^T$,

$\boldsymbol{u}_{c2} = [u_{ped} \quad u_{col}]^T$, $\boldsymbol{d}_{t2} = [d_{t7} \quad d_{t8} \quad d_{t9}]^T$, E_{11} is 3×3 identity matrix, Matrices $A_{11}, A_{21}, A_{22}, B_{11}, B_{22} \, C_1, C_2$, are given as

$$A_{11} = \begin{bmatrix} X_u & 0 & -g & 0 & 0 & 0 & 0 & 0 \\ 0 & Y_v & 0 & g & 0 & 0 & 0 & 0 \\ 0 & 0 & 0 & 0 & 1 & 0 & 0 & 0 \\ 0 & 0 & 0 & 0 & 0 & 1 & 0 & 0 \\ M_u & M_v & 0 & 0 & 0 & 0 & M_a & 0 \\ L_u & L_v & 0 & 0 & 0 & 0 & 0 & L_b \\ 0 & 0 & 0 & 0 & -1 & 0 & -1/t_f & A_b \\ 0 & 0 & 0 & 0 & 0 & -1 & B_a & -1/t_f \end{bmatrix}, \quad B_{11} = \begin{bmatrix} 0 & 0 \\ 0 & 0 \\ 0 & 0 \\ 0 & 0 \\ 0 & 0 \\ 0 & 0 \\ A_{lon} & A_{lat} \\ B_{lon} & B_{lat} \end{bmatrix},$$

$$C_1 = \begin{bmatrix} 1 & 0 \\ 0 & 1 \\ 0 & 0 \\ 0 & 0 \\ 0 & 0 \\ 0 & 0 \\ 0 & 0 \\ 0 & 0 \end{bmatrix}^T, \quad A_{21} = \begin{bmatrix} 0 & 0 & 0 & 0 & 0 & 0 & 0 & 0 \\ 0 & N_v & 0 & 0 & 0 & N_p & 0 & 0 \\ 0 & 0 & 0 & 0 & 0 & 0 & Z_a & Z_b \end{bmatrix}, \quad A_{22} = \begin{bmatrix} 0 & 1 & 0 \\ 0 & N_r & N_w \\ 0 & Z_r & Z_w \end{bmatrix},$$

$$B_{22} = \begin{bmatrix} 0 & 0 \\ N_{ped} & N_{col} \\ 0 & Z_{col} \end{bmatrix}, C_2 = \begin{bmatrix} 1 & 0 \\ 0 & 0 \\ 0 & 1 \end{bmatrix}^T$$

For hover operation, the DOB-SMC control law is only derived for the longitudinal–lateral subsystem and heading-heave dynamics are regulated at hover condition using PID controllers. The subsystem (6) is expanded as

$$\begin{aligned} \dot{u} &= X_u u - g\theta + d_{t1} \\ \dot{v} &= Y_v v + g\emptyset + d_{t2} \\ \dot{\theta} &= q + d_{t3} \\ \dot{\emptyset} &= p + d_{t4} \\ \dot{q} &= M_u u + M_v v + M_a a + d_{t5} \\ \dot{p} &= L_u u + L_v v + L_b b + d_{t6} \\ \dot{a} &= -q - 1/t_f . a + A_b . b + A_{lon} . u_{lon} + A_{lat} . u_{lat} \\ \dot{b} &= -p - 1/t_f . b + B_a . a + B_{lon} . u_{lon} + B_{lat} . u_{lat} \end{aligned} \tag{8}$$

$$y_1 = [u \, v]^T \tag{9}$$

where $X_u, Y_v, M_u, M_v, M_a, L_u, L_v$ and L_b are helicopter stability derivatives, $d_{ti} \, \forall \, i = 1, 2, \cdots 6$ is the total disturbance including both model mismatch and external disturbances acting at channel i.

c) Reduced Order Linearized Model

The flapping angles a and b of the main rotor can be approximated by the steady state dynamics of the main rotor as in [22]

$$a = -t_f q + t_f(A_b. b + A_{lon}. u_{lon} + A_{lat}. u_{lat} \tag{10}$$

$$b = -t_f p + t_f(B_a. a + B_{lon}. u_{lon} + B_{lat}. u_{lat}) \tag{11}$$

Solving (10) and (11) for a and b and then substituting a and b in (8) gives

$$\begin{aligned}
\dot{u} &= X_u u - g\theta + d_{t1} \\
\dot{v} &= Y_v v + g\emptyset + d_{t2} \\
\dot{\theta} &= q + d_{t3} \\
\dot{\emptyset} &= p + d_{t4} \\
\dot{q} &= M_u u + M_v v - M_p p - M_q q + M_{lon}. u_{lon} + M_{lat}. u_{lat} + d_{t5} \\
\dot{p} &= L_u u + L_v v - L_p p - L_q q + L_{lon}. u_{lon} + L_{lat}. u_{lat} + d_{t6}
\end{aligned} \tag{12}$$

where $M_q = t_f M_a$, $M_p = M_a t_f^2. A_b$, $M_{lon} = M_a. t_f(t_f A_b B_{lon} + A_{lon})$, $M_{lat} = M_a t_f(t_f A_b B_{lat} + A_{lat})$, $L_p = t_f L_b$, $L_q = L_b t_f^2. B_a$, $L_{lon} = L_b t_f(t_f B_a A_{lon} + B_{lon})$, $L_{lat} = L_b t_f(t_f B_a A_{lat} + B_{lat})$.

The reduced order linearized model (12) is written in state space form as follows

$$\dot{\boldsymbol{x}}_r = A_r \boldsymbol{x}_r + B_r \boldsymbol{u}_{c1} + E_r \boldsymbol{d}_{tr} \tag{13}$$

$$\boldsymbol{y}_r = C_r \boldsymbol{x}_r \tag{14}$$

where $\boldsymbol{x}_r = [u\ v\ \theta\ \emptyset\ q\ p\ ]^T$, $\boldsymbol{u}_{c1} = [u_{lon}\ \ u_{lat}]^T$, $\boldsymbol{d}_{tr} = [d_{t1}\ \ d_{t2}\ \ d_{t3}\ \ d_{t4}\ \ d_{t5}\ \ d_{t6}]^T$, E_r is 6×6 identity matrix; $\boldsymbol{y}_r$ is output vector; Matrices A_r, B_r and C_r are given as

$$A_r = \begin{bmatrix} X_u & 0 & -g & 0 & 0 & 0 \\ 0 & Y_v & 0 & g & 0 & 0 \\ 0 & 0 & 0 & 0 & 1 & 0 \\ 0 & 0 & 0 & 0 & 0 & 1 \\ M_u & M_v & 0 & 0 & -M_q & -M_p \\ L_u & L_v & 0 & 0 & -L_q & -L_p \end{bmatrix}, B_r = \begin{bmatrix} 0 & 0 \\ 0 & 0 \\ 0 & 0 \\ 0 & 0 \\ M_{lon} & M_{lat} \\ L_{lon} & L_{lat} \end{bmatrix}, C_r = \begin{bmatrix} 1 & 0 \\ 0 & 1 \\ 0 & 0 \\ 0 & 0 \\ 0 & 0 \\ 0 & 0 \end{bmatrix}^T$$

Assumption 1. The matrix pair $\boldsymbol{A}_r$ and $\boldsymbol{B}_r$ is controllable.
Assumption 2. The input derivatives M_{lon}, M_{lat}, L_{lon} and L_{lat} are nonzero.
Assumption 3. The stability derivatives g; M_a and L_b are nonzero.
Assumptions 1, 2 and 3 reflect the fact that the reduced order linearized model (13) is physically meaningful.
Assumption 4. The disturbance $d_{ti} \ \forall \ i = 1,2,\ldots,6$ acting at system (13) is continuous and satisfies

$$|d_{ti}| \leq \mu_i \tag{15}$$

where μ_i is positive bounded constant.
Assumption 5. The disturbance $d_{ti} \ \forall \ i = 1,2,\cdots,6$ belongs to a class of slow varying disturbances having constant value in steady state such that its derivative is bounded and satisfies $\lim_{t \to \infty} \dot{d}_{ti} = 0$.

Lemma 1: [23]. A nonlinear system $\dot{x} = f(x(t), w(t))$ is input to state stable (ISS). If it satisfies the condition when the input of the system goes to zero ($\lim_{t \to \infty} w(t) = 0$) then the states must go to zero ($\lim_{t \to \infty} x(t) = 0$).

3. DISTURBANCE OBSERVER DESIGN

It is difficult to measure directly the disturbances of the longitudinal-lateral subsystem (13), a linear disturbance observer is used to estimate the unknown total disturbance vector $\boldsymbol{d}_{tr}$. The DOB is designed as

$$\dot{\boldsymbol{P}} = -LE_r(\boldsymbol{P} + L\boldsymbol{x}_r) - L(A_r\boldsymbol{x}_r + B_r\boldsymbol{u}_{c1}) \tag{16}$$

$$\widehat{\boldsymbol{d}}_{tr} = \boldsymbol{P} + L\boldsymbol{x}_r \tag{17}$$

where $\widehat{\boldsymbol{d}}_{tr} = [\hat{d}_{t1} \quad \hat{d}_{t2} \quad \hat{d}_{t3} \quad \hat{d}_{t4} \quad \hat{d}_{t5} \quad \hat{d}_{t6}]^T$ is the disturbance estimation vector, $\boldsymbol{P}$ is a 6×1 auxiliary vector and $L = diag(l_1, l_2, l_3, l_4, l_5, l_6)$ is observer gain.

Theorem 1. Suppose system (13) satisfies Assumptions 4 and 5. The disturbance estimation vector $\widehat{\boldsymbol{d}}_{tr}$ of DOB can asymptotically track the total lumped disturbance vector $\boldsymbol{d}_{tr}$ if the observer gain matrix L is chosen such that $-L$ is Hurwitz.
Proof. The estimation error of the DOB is defined as

$$\boldsymbol{e}_d = \widehat{\boldsymbol{d}}_{tr} - \boldsymbol{d}_{tr} \tag{18}$$

$$\boldsymbol{e}_d = [e_{dt1} \quad e_{dt2} \quad e_{dt3} \quad e_{dt4} \quad e_{dt5} \quad e_{dt6}]^T \tag{19}$$

Differentiating (17) gives

$$\dot{\widehat{\boldsymbol{d}}}_{tr} = \dot{\boldsymbol{P}} + L\dot{\boldsymbol{x}}_r \tag{20}$$

$$\dot{\widehat{\boldsymbol{d}}}_{tr} = -L\boldsymbol{e}_d \tag{21}$$

$$\dot{\widehat{\boldsymbol{d}}}_{tr} = -[L_1\boldsymbol{e}_{d1} \quad L_2\boldsymbol{e}_{d2} \quad L_3\boldsymbol{e}_{d3}]^T \tag{22}$$

where $\boldsymbol{e}_{d1} = [e_{dt1} \quad e_{dt2}]^T$, $\boldsymbol{e}_{d2} = [e_{dt3} \quad e_{dt4}]^T$, $\boldsymbol{e}_{d1} = [e_{dt5} \quad e_{dt6}]^T$, $L_1 = diag(l_1, l_2)$, $L_2 = diag(l_3, l_4)$ and $L_3 = diag(l_5, l_6)$.
Differentiating (18) and substituting (21) gives

$$\dot{\boldsymbol{e}}_d = -L\boldsymbol{e}_d - \dot{\boldsymbol{d}}_{tr} \tag{23}$$

The error system (23) is asymptotically stable since $-L$ is Hurwitz and $\dot{\boldsymbol{d}}_{tr}$ satisfies Assumption 5. This proves that the disturbance estimation vector $\widehat{\boldsymbol{d}}_{tr}$ tracks the total disturbance $\boldsymbol{d}_{tr}$ of system (13) asymptotically. Considering Lemma 1 it is also verified that the error system (23) is ISS.

Assumption 6. The estimation error of DOB is bounded such that

$$e_{dti}^* = \max_{t>0}|e_{dti}| \ \forall \ i = 1,2,\cdots,6 \tag{24}$$

4. DOB-SMC at hover

(a) Input-output feedback linearization

To derive the proposed control law for hover operation, first the helicopter reduced dynamics (13) is input-output feedback linearized. The system output (14) is simplified as

$$y_r = \begin{bmatrix} u \\ v \end{bmatrix} \tag{25}$$

Differentiating y_r gives

$$\dot{y}_r = K_1 \begin{bmatrix} u \\ v \end{bmatrix} + K_2 \begin{bmatrix} \theta \\ \emptyset \end{bmatrix} + d_{tr1} \tag{26}$$

where $K_1 = diag(X_u, Y_v)$, $K_2 = diag(-g, g)$ and $d_{tr1} = [d_{t1} \quad d_{t2}]^T$.
Differentiating (26) and taking $\dot{d}_{tr1} = 0$ (assumption 5) gives

$$\ddot{y}_r = K_1^2 \begin{bmatrix} u \\ v \end{bmatrix} + K_1 K_2 \begin{bmatrix} \theta \\ \emptyset \end{bmatrix} + K_2 \begin{bmatrix} q \\ p \end{bmatrix} + K_1 d_{tr1} + K_2 d_{tr2} \tag{27}$$

where $d_{tr2} = [d_{t3} \quad d_{t4}]^T$. Differentiating (27) and taking $\dot{d}_{tr1}$ and $\dot{d}_{tr2}$ as zero results

$$\dddot{y}_r = K_1^3 \begin{bmatrix} u \\ v \end{bmatrix} + K_1^2 K_2 \begin{bmatrix} \theta \\ \emptyset \end{bmatrix} + K_1 K_2 \begin{bmatrix} q \\ p \end{bmatrix} + K_2 K_3 \begin{bmatrix} u_{lon} \\ u_{lat} \end{bmatrix} + K_2 K_4 [u \quad v \quad q \quad p]^T \\ + K_1^2 d_{tr1} + K_1 K_2 d_{tr2} + K_2 d_{tr3} \tag{28}$$

where

$$K_3 = \begin{bmatrix} M_{lon} & M_{lat} \\ L_{lon} & L_{lat} \end{bmatrix}, K_4 = \begin{bmatrix} M_u & M_v & -M_q & -M_p \\ L_u & L_v & -L_p & -L_q \end{bmatrix}, d_{tr3} = \begin{bmatrix} d_{t5} \\ d_{t6} \end{bmatrix}$$

(b) Controller design

In this section, DOB-SMC method is used to derive control law to stabilize helicopter at hover condition in presence of external disturbances. The sliding surface augmented with the estimated disturbances is designed as follows

$$S = C_1 y_r + C_2 \hat{\dot{y}}_r + \hat{\ddot{y}}_r \tag{29}$$

where $S = [s_1 \quad s_2]^T$, $C_1 = diag(c_1, c_2)$, $C_2 = diag(c_3, c_4)$. C_1 and C_2 are designed such that $S = 0$ is Hurwitz. $\hat{\dot{y}}_r$ and $\hat{\ddot{y}}_r$ are expressed as follows

$$\hat{\dot{y}}_r = K_1 \begin{bmatrix} u \\ v \end{bmatrix} + K_2 \begin{bmatrix} \theta \\ \emptyset \end{bmatrix} + \hat{d}_{tr1} \tag{30}$$

$$\hat{\ddot{y}}_r = K_1^2 \begin{bmatrix} u \\ v \end{bmatrix} + K_1 K_2 \begin{bmatrix} \theta \\ \emptyset \end{bmatrix} + K_2 \begin{bmatrix} q \\ p \end{bmatrix} + K_1 \hat{d}_{tr1} + K_2 \hat{d}_{tr2} \tag{31}$$

where $\hat{d}_{tr1} = [\hat{d}_{t1} \quad \hat{d}_{t2}]^T$ and $\hat{d}_{tr2} = [\hat{d}_{t3} \quad \hat{d}_{t4}]^T$.

The proposed DOB-SMC for the helicopter hover operation is designed as follows

$$u_{c1} = (-K_2 K_3)^{-1} \big(h + C_1 \hat{d}_{tr1} + C_2 (K_1 \hat{d}_{tr1} + K_2 \hat{d}_{tr2}) + K_1^2 \hat{d}_{tr1} + K_1 K_2 \hat{d}_{tr2} \\ + K_2 \hat{d}_{tr3} + \beta sgn(S) + \gamma S \big) \tag{32}$$

where $\beta = diag(\beta_1, \beta_2)$; $\gamma = diag(\gamma_1, \gamma_2)$; $sgn(S) = [sgn(s_1) \quad sgn(s_2)]^T$ and $\hat{d}_{tr3} = [\hat{d}_{t5} \quad \hat{d}_{t6}]^T$, and

$$\boldsymbol{h} = C_1 \left(K_1 \begin{bmatrix} u \\ v \end{bmatrix} + K_2 \begin{bmatrix} \theta \\ \emptyset \end{bmatrix} \right) + C_2 \left(K_1^2 \begin{bmatrix} u \\ v \end{bmatrix} + K_1 K_2 \begin{bmatrix} \theta \\ \emptyset \end{bmatrix} + K_2 \begin{bmatrix} q \\ p \end{bmatrix} \right) + K_1^3 \begin{bmatrix} u \\ v \end{bmatrix}$$
$$+ K_1^2 K_2 \begin{bmatrix} \theta \\ \emptyset \end{bmatrix} + K_1 K_2 \begin{bmatrix} q \\ p \end{bmatrix} + K_2 K_4 [u \quad v \quad q \quad p]^T \tag{33}$$

(c) Stability Analysis

Theorem 2. Suppose system (13) satisfy assumptions 5 and 6 then system (13) under the proposed control law (32) is asymptotically stable if the high frequency switching gain in the control law is designed such that following two conditions hold

$$\beta_1 > |([1 \quad 0]M^*)| \tag{34}$$

and

$$\beta_2 > |([0 \quad 1]M^*)| \tag{35}$$

where $\quad M^* = -[C_1 + K_1^2 + C_2 K_1 + (C_2 + K_1)L_1]\boldsymbol{e}_{d1}^* - [C_2 K_2 + K_1 K_2 + K_2 L_2]\boldsymbol{e}_{d2}^* - K_2 \boldsymbol{e}_{d3}^*$, $\boldsymbol{e}_{d1}^* = [e_{dt1}^* \quad e_{dt2}^*]^T$, $\boldsymbol{e}_{d2}^* = [e_{dt3}^* \quad e_{dt4}^*]^T$ and $\boldsymbol{e}_{d3}^* = [e_{dt5}^* \quad e_{dt6}^*]^T$.

Proof. Differentiating the sliding surface (29) gives

$$\dot{\boldsymbol{S}} = \boldsymbol{h} + K_2 K_3 \boldsymbol{u}_{c1} + C_1 \boldsymbol{d}_{tr1} + C_2 (K_1 \boldsymbol{d}_{tr1} + K_2 \boldsymbol{d}_{tr2} + \dot{\hat{\boldsymbol{d}}}_{tr1}) + K_1^2 \boldsymbol{d}_{tr1} + K_1 K_2 \boldsymbol{d}_{tr2}$$
$$+ K_2 \boldsymbol{d}_{tr3} + K_1 \dot{\hat{\boldsymbol{d}}}_{tr1} + K_2 \dot{\hat{\boldsymbol{d}}}_{tr2} \tag{36}$$

Substituting the control law (32) in (36) gives

$$\dot{\boldsymbol{S}} = -(C_1 + K_1^2 + C_2 K_1)\boldsymbol{e}_{d1} - (C_2 K_2 + K_1 K_2)\boldsymbol{e}_{d2} - K_2 \boldsymbol{e}_{d3} + (C_2 + K_1)\dot{\hat{\boldsymbol{d}}}_{tr1}$$
$$+ K_2 \dot{\hat{\boldsymbol{d}}}_{tr2} - \beta sgn(\boldsymbol{S}) - \gamma \boldsymbol{S} \tag{37}$$

Substituting $\dot{\hat{\boldsymbol{d}}}_{tr1}$ and $\dot{\hat{\boldsymbol{d}}}_{tr2}$ from (22) in (37) gives

$$\dot{\boldsymbol{S}} = -[C_1 + K_1^2 + C_2 K_1 + (C_2 + K_1)L_1]\boldsymbol{e}_{d1} - [C_2 K_2 + K_1 K_2 + K_2 L_2]\boldsymbol{e}_{d2} - K_2 \boldsymbol{e}_{d3}$$
$$- \beta sgn(\boldsymbol{S}) - \gamma \boldsymbol{S} \tag{38}$$

$$\dot{\boldsymbol{S}} = M - \beta sgn(\boldsymbol{S}) - \gamma \boldsymbol{S} \tag{39}$$

where M is bounded by M^*.
Now defining the candidate Lyapunov function as

$$V = \frac{1}{2}\boldsymbol{S}^T \boldsymbol{S} \tag{40}$$

Differentiating (40) and substituting (39) gives

$$\dot{V} = ([1 \quad 0]M)s_1 + ([0 \quad 1]M)s_2 - \beta_1 |s_1| - \beta_2 |s_2| - \gamma_1 s_1^2 - \gamma_2 s_2^2 \tag{41}$$

Using the conditions (34) and (35) it is concluded that

$$\dot{V} < 0 \quad \forall \boldsymbol{S} \neq \boldsymbol{0} \tag{42}$$

So it is proved that the system states will reach the defined sliding surface $\boldsymbol{S} = 0$ in finite time. At condition $S = 0$, (29) becomes

$$\hat{\dot{\boldsymbol{y}}}_r = -C_1 \boldsymbol{y}_r - C_2 \hat{\dot{\boldsymbol{y}}}_r \tag{43}$$

Substituting (30) and (31) in (43) gives

$$\ddot{\boldsymbol{y}} = -[C_1 \boldsymbol{y} + C_2 \dot{\boldsymbol{y}} + (K_1 + C_2)\boldsymbol{e}_{d1} + K_2 \boldsymbol{e}_{d2}] \tag{44}$$

Combining (44) with DOB error dynamics (23) yields

$$\ddot{\boldsymbol{y}} = -[C_1 \boldsymbol{y} + C_2 \dot{\boldsymbol{y}} + (K_1 + C_2)\boldsymbol{e}_{d1} + K_2 \boldsymbol{e}_{d2}]$$
$$\dot{\boldsymbol{e}}_d = -L\boldsymbol{e}_d - \dot{\boldsymbol{d}}_{tr} \tag{45}$$

Let

$$\boldsymbol{\varepsilon} = [\boldsymbol{\varepsilon}_1 \quad \boldsymbol{\varepsilon}_2 \quad \boldsymbol{\varepsilon}_3 \quad \boldsymbol{\varepsilon}_4 \quad \boldsymbol{\varepsilon}_5] = [\boldsymbol{y} \quad \dot{\boldsymbol{y}} \quad \boldsymbol{e}_{d1} \quad \boldsymbol{e}_{d2} \quad \boldsymbol{e}_{d3}]$$

then (45) is written as

$$\dot{\boldsymbol{\varepsilon}} = A_\varepsilon \boldsymbol{\varepsilon} + B_\varepsilon \dot{\boldsymbol{d}}_{tr} \tag{46}$$

where A_ε and B_ε are given as

$$A_\varepsilon = \begin{bmatrix} 0 & 1 & \vdots & 0 & 0 & 0 \\ -C_1 & -C_2 & \vdots & -(K_1 + C_2) & -K_2 & 0 \\ \dots & \dots\dots & \dots\dots & \dots\dots\dots\dots\dots & \dots\dots & \dots \\ 0 & 0 & \vdots & & -L & \end{bmatrix}, \quad B_\varepsilon = \begin{bmatrix} 0_{4\times4} \\ I_{6\times6} \end{bmatrix}$$

So it is verified that the matrix A_ε is Hurwitz as $-L$ and sliding surface $\boldsymbol{S}$ are Hurwitz, which means the system $\dot{\varepsilon} = A_\varepsilon \varepsilon$ is exponentially stable and the proposed control law (32) guarantees that the states of the system (13) during sliding phase will move to equilibrium point asymptotically. Considering Assumption 5 and Lemma 1 it is verified that system (46) is ISS.

5. SIMULATION RESULTS

In this section evaluation of the proposed controller (32) is presented. Performance of (32) is compared with a traditional sliding mode control (SMC) to get a clear idea of its efficiency. The sliding surface of the traditional SMC method is designed as

$$\boldsymbol{\sigma} = C_1 \boldsymbol{y}_r + C_2(\dot{\boldsymbol{y}}_r - \boldsymbol{d}_1) + \ddot{\boldsymbol{y}}_r - K_1 \boldsymbol{d}_1 - K_2 \boldsymbol{d}_2 \tag{47}$$

Substituting $\dot{\boldsymbol{y}}_r$ and $\ddot{\boldsymbol{y}}_r$ in (47) the disturbance terms $\boldsymbol{d}_1$ and $K_1 \boldsymbol{d}_1 + K_2 \boldsymbol{d}_2$ get cancelled. So it's a typical sliding surface designed to control the linearized model (13) without considering the disturbance vector $\boldsymbol{d}_{tr}$.
Then the traditional SMC is designed as

$$\boldsymbol{u} = (-K_2 K_3)^{-1}(\boldsymbol{h} + \beta sgn(\boldsymbol{\sigma})) \tag{48}$$

Using DOB there is initial peaking at time t_0 in disturbance approximation which causes higher control gain and even can takes the control input to saturation.
This initial peaking in disturbance approximation is directly proportional to the observer gain L. Hence to avoid the initial peaking phenomena the observer gain L is designed as follows

$$\boldsymbol{u} = L = \begin{cases} \sin(\pi t/2) \, QI, & 0 \le t \le 1 \\ QI, & t > 1 \end{cases} \tag{49}$$

where Q is any positive number and I 6×6 identity matrix. So L is zero at t_0 and positive elsewhere it satisfies the condition that $-L$ Hurwitz.

Raptor 90 SE radio controlled helicopter is used in these simulations.

The Simulink model is established using the nonlinear model of helicopter defined in (1) and then the proposed DOB-SMC (32) and the traditional SMC (48) based on the linearized model (13) are applied on it to check the hovering performance of helicopter in presence of wind disturbance.

Parameters of the nonlinear model of the helicopter are given in table 1 and parameters of the reduced order linearized model (13) are given in Table 2.

Table 1. Parameters of Raptor 90SE RC helicopter [24]

Nonlinear model parameters	
$m = 7.495\ kg$	$\Omega = 172.788$ rad/s
$R = 0.785\ m$	$N_v = 2.982$
$b_m = 2$	$N_p = 0$
$c_m = 0.060$ m	$N_w = -0.7076$
$\rho = 1.290$ kg/m^3	$N_r = -10.71$
$g = 9.81\ m/s^2$	$N_{ped} = 26.90$
$C_{l\alpha}^m = 4.0734$	$N_{col} = 3.749$
$k_a = 9.4248$	$t_f = 0.03256\ sec$
$k_{col} = 0.3813$	$A_b = 0.7713$
$k_\beta = 167.6592$ N. m/rad	$B_a = 0.6168$
$h_{mr} = 0.275$ m	$A_{lon} = 4.059$
$I_{xx}\ =\ 0.1895\ kg\ m^2$	$A_{lat} = -0.01610$
$I_{yy}\ =\ 0.4515\ kg\ m^2$	$B_{lon} = -0.01017$
$I_{zz}\ =\ 0.3408\ kg\ m^2$	$B_{lat} = 4.085$

Table 2. Parameters of the linearized model [15]

A_r Matrix	
$X_u = -0.03996$	$Y_v = -0.05989$
$M_u = 0.2542$	$M_v = -0.06013$
$L_u = -0.0244$	$L_v = -0.1173$
$M_q = 10.0153$	$M_p = 0.2515$
$L_q = 0.7667$	$L_p = 38.1792$
B_r Matrix	
$M_{lon} = 40.6609$	$M_{lat} = 0.8662$
$L_{lon} = 2.7238$	$L_{lat} = 155.9401$

Table 3. Controller parameters

Controller	Parameters
SMC	$c_1 = 10, c_2 = 10, c_3 = 25, c_4 = 25$ $\beta_1 = 10, \beta_2 = 10$
DOB-SMC	$c_1 = 10, c_2 = 10, c_3 = 25, c_4 = 25$ $\beta_1 = 10, \beta_2 = 10\ \ Q = 10$

a) Case: 1. Performance Comparison

First performance of the two controllers DOB-SMC and SMC is done in absence of external disturbance.

The initial states of helicopter system (1) are set as $u = 1$ and $v = -1$ the rest of the states are zero initially.

The controller parameters are given in table III. It is observed from Fig. 2 that DOB-SMC has better settling time compared to the traditional SMC.

In Fig. 3 it is showed that DOB-SMC has higher initial control gain which is the reason for quick settling time while in steady-state chatter in control input is same in both controllers. Fig. 4 shows that the approximated mismatched disturbances $(d_{t1}, d_{t2}, d_{t3}, d_{t4})$ goes to zero as soon as all the states of the system reach zero as there was no external disturbance applied on the system.

There is small scale matched disturbances (d_{t5}, d_{t6}) in steady state due to the model mismatch caused by order reduction.
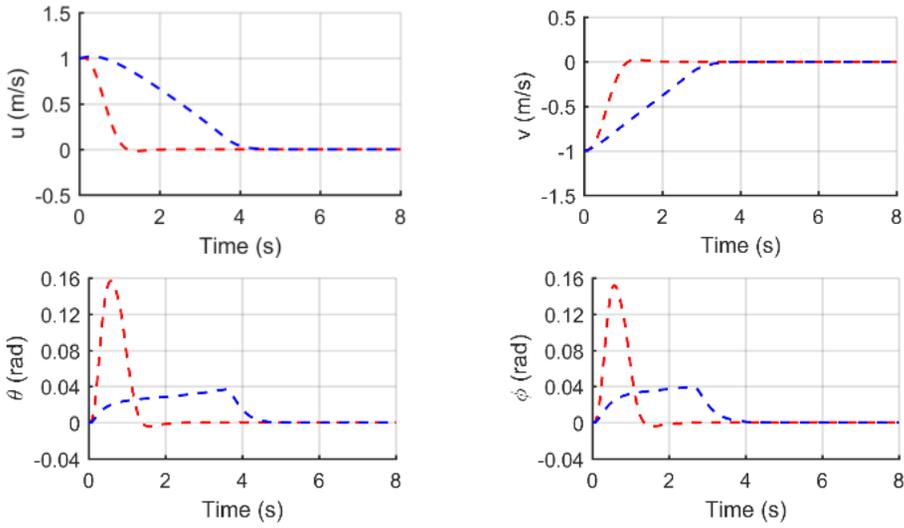
Figure 2. State variable in case1. Red line shows DOB-SMC, Blue line shows Traditional SMC
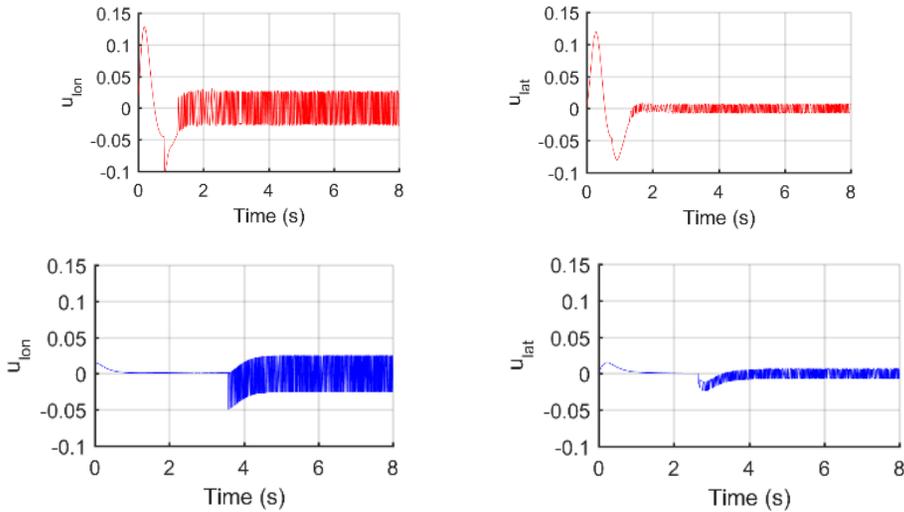
Figure 3. Control input in case1. Redline shows DOB-SMC, blue line shows Traditional SMC
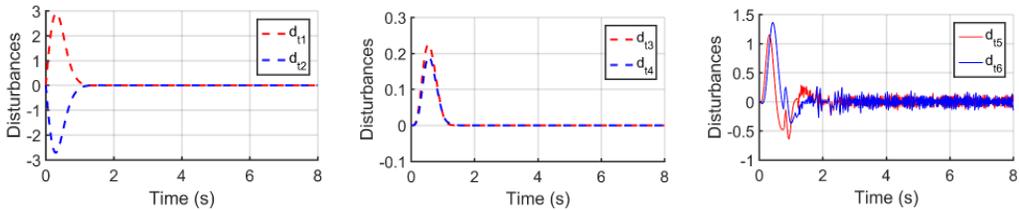
Figure 4. Disturbances approximated by DOB in case 1

b) Case: 2. Handling Mismatch Uncertainties

In second case to compare the mismatched uncertainty handling capacity of both controllers, external wind disturbances d_{w1} and d_{w2} are applied on the helicopter system (1) defined as

$$d_{w1} = d_{w2} = d_w = \begin{cases} 0, & 0 \leq t \leq 1 \\ 1, & t > 1 \end{cases} \qquad (50)$$

Control parameters are same as defined in table III except β_1 and β_2 which are increased to 30 in both controllers. All initial state are zero. In Fig. 5 it is observed that DOB-SMC suppress the external wind disturbances and bring back u and v to zero but traditional SMC failed to bring back the states u and v to desired equilibrium and there is a large constant steady state error. This confirm that traditional SMC is sensitive to mismatched uncertainties. Fig. 7 shows that external wind disturbances are perfectly approximated by DOB and d_{t1} and d_{t2} goes to d_w in short time.
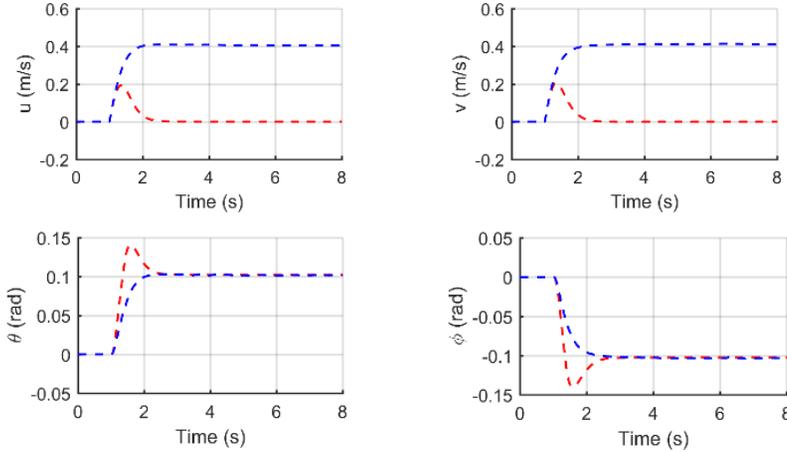
Figure 5. State variable in case2. Red line shows DOB-SMC, Blue line shows Traditional SMC
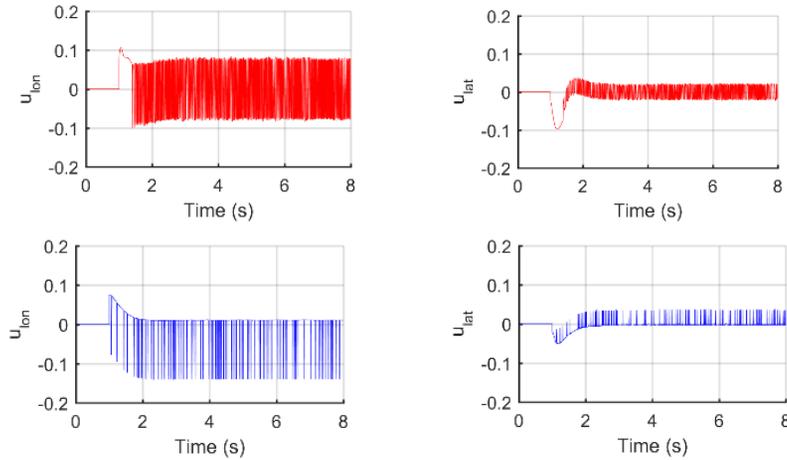
Figure 6. Control input in case2. Redline shows DOB-SMC, blue line shows Traditional SMC
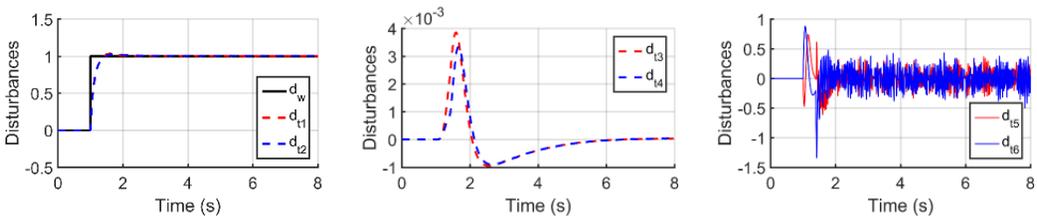
Figure 7. Disturbances approximated by DOB in case 2

c) **Case: 3. Chatter Reduction**

In third case we reduce β_1 and β_2 back to 10 and all control parameters are same as defined in table III. Disturbances (50) are applied in the same way as in case 2. Fig. 8. Shows that DOB-SMC still suppressed mismatch disturbances and brought back u and v to zero with a slight increase in settling time but traditional SMC failed to keep the state of the system bounded. In this case the high frequency switching gain is decreased three times and as shown in Fig. 9 the control input chatter is much smaller than that in case two(Fig. 6). Fig. 10 shows that the mismatched disturbances approximated by DOB and are same as in case 2.
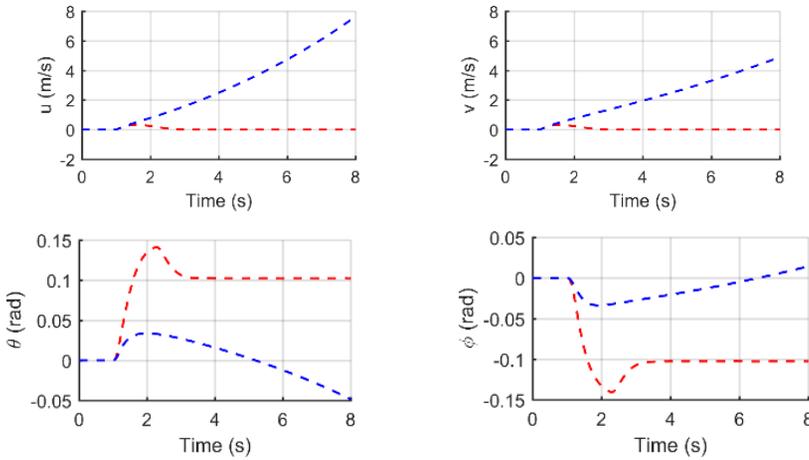
Figure 8. State variable in case3. Red line shows DOB-SMC, Blue line shows Traditional SMC
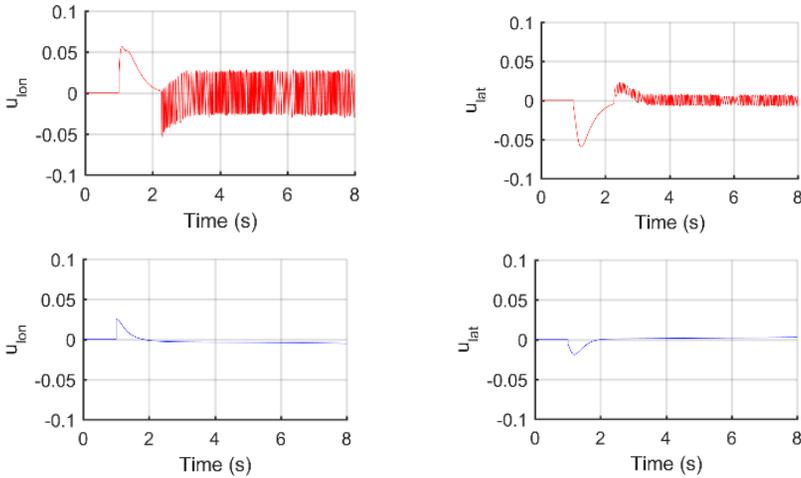
Figure 9. Control input in case3. Redline shows DOB-SMC, blue line shows Traditional SMC
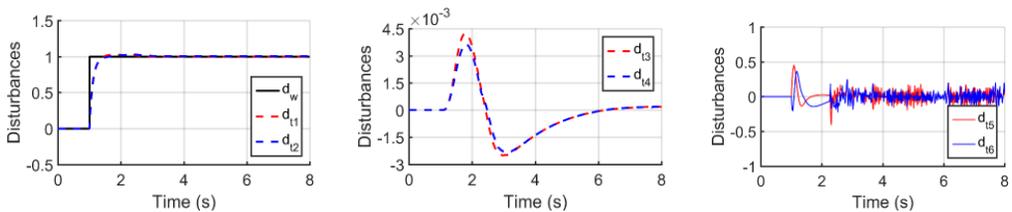
Figure 10. Disturbances approximated by DOB in case 3

6. CONCLUSIONS

This paper presents DOB-SMC design based on the linearized model of the helicopter at hover condition. The designed controller is applied to a complete nonlinear model of the helicopter (Raptor 90 SE). Simulation results showed that DOB accurately estimates the model mismatch and external disturbances and the proposed DOB-SMC method is capable of stabilizing the helicopter during hover operations in presence of external disturbances. Comparison of DOB-SMC with traditional SMC showed superior performance.

REFERENCES

[1] J. G. Leishman, *Principles of Helicopter Aerodynamics,* Cambridge University Press, 2006.

[2] H. Shim, T. Koo, F. Hoffmann, et al, *A comprehensive study of control design for an autonomous helicopter*: In Proceedings of the 37th IEEE Conference on Decision and Control, Vol **4**, pp. 3653–3658, 1998.

[3] E. N. Sanchez, H. M. Becerra, C. M. Velez, *Combining fuzzy pid and regulation control for an autonomous minihelicopter*, Information Sciences, Vol **177**, pp.1999–2022, 2007

[4] E. Lee, H. Shim, H. Park, et al. *Design of hovering attitude controller for a model helicopter*: In Proceedings of society of instrument and control engineers, 1385-1389, Tokyo, 1993.

[5] M. L. Civita, George Papageorgiou, William Messner, et al., *Design and flight testing of a high-bandwidth h-infinity loop shaping controller for a robotic helicopter*: In, AIAA Guidance, Navigation, and Control Conference and Exhibit, California, pp. 4836, 2002

[6] B. Guerreiro, C. Silvestre, R. Cunha, et al. *Trajectory tracking H2 controller for autonomous helicopters: An application to industrial chimney inspection*, In 17th IFAC Symposium on Automatic Control in Aerospace, 431-436, Toulouse, France 2007.

[7] J. Gadewadikar, F. Lewis, K. Subbarao, et al., Structured H∞ command and control-loop design for unmanned helicopters, *Journal of Guidance, Control, and Dynamics*, Vol **31**, pp. 1093–1102, 2008.

[8] I. B. Tijani, R. Akmeliawati, A. Legowo, H-infinity robust controller for autonomous helicopter hovering control, *Aircraft engineering & aerospace technology*, Vol **83**, pp. 363–374, 2011.

[9] M. F. Weilenmann, H. P. Geering, *A test bench for rotorcraft hover control*: In AIAA Guidance, Navigation and Control Conference, pp. 1371–1382, USA, 1993.

[10] M. F. Weilenmann, U. Christen, H. P. Geering, *Robust helicopter position control at hover:* In American Control Conference, pp. 2491-2495, Maryland USA, 1999.

[11] S. Li, J. Yang, W. Chen, X. Chen, *Disturbance Observer-Based Control: Methods and Applications*. CRC Press, 2014.

[12] L. Besnard, Y.B. Shtessel, B. Landrum, *Control of a quadrotor vehicle using sliding mode disturbance observer*: In American Control Conference, 2007.

[13] C. Fan, S. Guo, D. Li, *Nonlinear predictive attitude control with a disturbance observer of an unmanned helicopter on the test bench*: In IEEE 5th International Conference on Robotics, Automation and Mechatronics, pp. 304-309, Qingdao China, 2011.

[14] D. C. Robinaon, K. Ryan, H. Chung, *Helicopter hovering attitude control using a direct feedthrough Simultaneous state and disturbance Observer*, In IEEE Conference on Control Applications, pp. 633-638 Sydney Australia, 2015.

[15] I. A. Raptis, K. P. Valavanis. *Velocity and heading tracking control for small-scale unmanned helicopters*, In American control conference, pp. 1579–1586, San Francisco, USA, 2011.

[16] I. A. Raptis, K. P. Valavanis, G. J Vachtsevanos, *Linear tracking control for small-scale unmanned helicopters*, IEEE Trans Control Syst Technol, Vol **20**, pp. 995–1010, 2012.

[17] J. Yang, S. Li, X. Yu. *Sliding-mode control for systems with mismatched uncertainties via a disturbance observer*, IEEE Transactions on Industrial Electronics, Vol **60**, pp. 160–169, 2013.

[18] X. Bin, G. Jianchuan, Z. Yao, Z. Bo, Sliding mode tracking control for miniature unmanned helicopters, *Chinese Journal of Aeronautics*, Vol **28**, pp. 277–284, 2015.

[19] A. Budiyono, S. S. Wibowo, Optimal tracking controller design for a small scale helicopter, *Journal of Bionic Engineering*, Vol **4**, pp. 272–279, 2007.

[20] V. Gavrilets, *Dynamic model for a miniature aerobatic helicopter*, Handbook of Unmanned Aerial Vehicles, Springer, pp. 279–306, 2015.

[21] S. Tang, L. Zhang, S. Qian, Z Zheng, Second-order sliding mode attitude controller design of a small-scale helicopter, *Science China Information Sciences*, Vol. **59**, pp. 112209-14, 2016.

[22] C. Liu, W. H. Chen, and J. Andrews, Tracking control of small-scale helicopters using explicit nonlinear MPC augmented with disturbance observers, *Control Engineering Practice*, Vol **20**, pp. 258–268, 2012.

[23] H. K. Khalil, *Nonlinear systems, 2nd edition*, Upper Saddle River, NJ:Prentice Hall, 1996.

[24] S. Tang, Z. Zheng, S. Qian, X Zhao, Nonlinear system identification of a small-scale unmanned helicopter, *Control Engineering Practice*, Vol **25**, pp. 1–15, 2014.